III-3

Chemistry

BL1U

Tracking Few-Femtosecond Auger Decay by Synchrotron Radiation

T. Kaneyasu[1], Y. Hikosaka[2], M. Fujimoto[3,4], H. Iwayama[3,4] and M. Katoh[5,3]

[1]SAGA Light Source, Tosu 841-0005, Japan
[2]Institute of Liberal Arts and Sciences, University of Toyama, Toyama 930-0194, Japan
[3]UVSOR Synchrotron Facility, Institute for Molecular Science, Okazaki 444-8585, Japan
[4]The Graduate University for Advanced Studies, SOKENDAI, Okazaki 444-8585, Japan
[5]Hiroshima Synchrotron Radiation Center, Hiroshima University, Higashi-Hiroshima 739-0046, Japan

The sequential interaction of a pair of time-separated pulses with an atomic or molecular system results in quantum interference between the resulting atomic/molecular wave packets. In this work, we use the recently disclosed ability of synchrotron light sources to perform wave packet interferometry experiments [1,2]. By using soft x-ray radiation wave packets with attosecond-controlled spacing, we observed the time-domain interferogram due to the interference between electron wave packets launched from the inner-shell 4d orbital of the Xe atom [3]. The time-domain approach presented here enables us to control the quantum interference in atomic inner-shell processes and to track the femtosecond decay of the short-lived excited state.

The experiment was carried out at beamline BL1U. The light source of BL1U consists of twin APPLE-II undulators. The electrons passing through the undulators emit pairs of 10-cycle radiation wave packets [Fig. 1]. The temporal duration and spectral width of the radiation wave packets were about 2 fs and 3 %, respectively. The peak photon energy of the 3rd harmonic radiation was adjusted close to the energy of the $4d_{5/2}^{-1}6p$ resonance. In order to monitor the population of the $4d_{5/2}^{-1}6p$ excited state, we detected visible fluorescence photons of 460-nm-wavlength emitted from singly-charged ionic states formed via spectator resonant Auger decay.

Figure 2(a) shows the fluorescence yields measured as a function of time delay over a range from 0 to 21 fs. The time spectrum shows rapid oscillations, with a period of approximately 63 as. This can be understood as "time-domain Ramsey fringes", which arise from the quantum interference of electron wave packets launched at different times. Here the oscillation period corresponds to the transition frequency of the Xe $4d_{5/2}^{-1}6p$ inner-shell excited state.

It is clear that the amplitude of the Ramsey fringes decreases with increasing time delay. This can be explained by considering the time evolution of the first electron wave packet during the sequential interaction. Assuming a 6 fs lifetime for the $4d_{5/2}^{-1}6p$ state, the time-damped Ramsey fringe spectrum can be calculated. Figure 2(b) shows the calculated spectrum, taking into account the temporal resolution of the delay control. The good agreement between experiment and calculation confirms that the reduction in fringe amplitude does indeed arise from the excited state

lifetime, proving the time-domain access to femtosecond Auger decay processes. While the temporal resolution in synchrotron experiments has been thought to be limited by the electron bunch length, the present study clearly shows that processes in much shorter timescale can be accessed by the use of the longitudinal coherence between radiation wave packets.
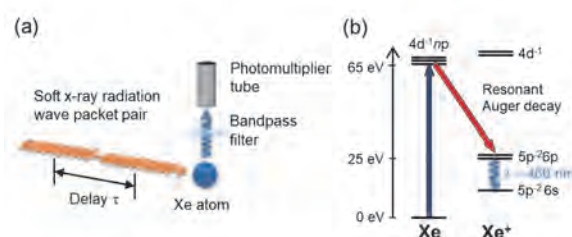

Fig. 1. (a) Experimental scheme for wave packet interferometry. (b) Energy level diagram of Xe atom.
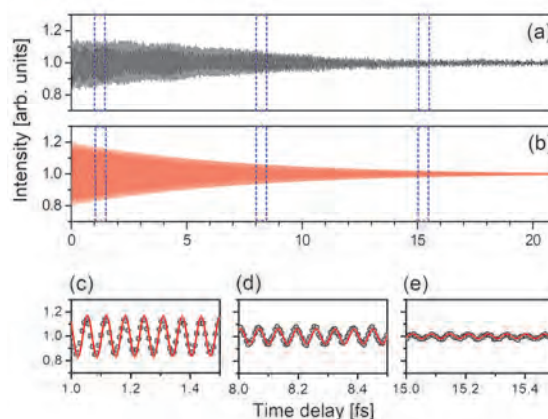

Fig. 2. (a) Fluorescence yield measured as a function of time delay. (b) Calculated spectrum. (c)-(e) Comparison between the experimental and calculated spectra.

[1] Y. Hikosaka et al., Nat. Commun. 10 (2019) 4988.
[2] T. Kaneyasu et al., Phys. Rev. Lett. 123 (2019) 233401.
[3] T. Kaneyasu et al., Phys. Rev. Lett. 126 (2021) 113202.

BL1U

Polarization Control in a Crossed-Undulator without a Monochromator

T. Kaneyasu[1], Y. Hikosaka[2], M. Fujimoto[3,4], H. Iwayama[3,4] and M. Katoh[5,3]

[1]SAGA Light Source, Tosu 841-0005, Japan
[2]Institute of Liberal Arts and Sciences, University of Toyama, Toyama 930-0194, Japan
[3]UVSOR Synchrotron Facility, Institute for Molecular Science, Okazaki 444-8585, Japan
[4]The Graduate University for Advanced Studies, SOKENDAI, Okazaki 444-8585, Japan
[5]Hiroshima Synchrotron Radiation Center, Hiroshima University, Higashi-Hiroshima 739-0046, Japan

The crossed undulator scheme for synchrotron radiation is a powerful method to produce light beams of various polarization states. In this study, we demonstrate that the polarization control of light from a crossed undulator can be achieved using the material response, without any prior monochromatization [1].

Figure 1 compares the polarization control of light from a crossed undulator by a conventional system and by the present method. A relativistic electron that passes though the undulators emits a pair of horizontally and vertically polarized radiation wave packets which are separated by time delay τ. In a conventional system, the radiation wave packets are temporally stretched by a monochromator which allows an interference between the two radiation fields. Various polarization states can be obtained by tuning the time delay using a phase shifter magnet that controls the electron orbit between the two undulators. On the other hand, when an atom is directly irradiated by non-monochromatized radiation from the crossed undulator, it absorbs specific frequency component. Therefore, the resonant photoabsorption is expected to reflect the polarization determined by the interference of radiation fields at the resonant frequency.

A proof-of-concept experiment was performed at BL1U. The light source of BL1U comprises a twin APPLE-II undulators. The upstream and downstream undulators were set in the vertical and horizontal linear polarizations, respectively. The UVSOR-III synchrotron was operated in the single bunch mode during the measurements. The non-monochromatized undulator radiation interacted with He atoms. The polarization property of the light was investigated by observing the Zeeman quantum beat in the fluorescence decay of the 1s6p ^{1}P excited state [2]. Fluorescence photons with a wavelength of 345 nm, which were emitted by the decay from 1s6p to 1s2s states, were detected using a photomultiplier tube equipped with a bandpass filter.

Figure 2 shows the fluorescence decay curves measured at different setting of time delay. The corresponding phase difference between the radiation fields was tuned from π to 9π/2 with a step of approximately π/2. The shapes of beat structures change according to the phase difference, reflecting the polarization state of light. The observed beat structures are well reproduced by the calculation curves. This result verifies that polarization control in the crossed undulator can be achieved using atomic response.
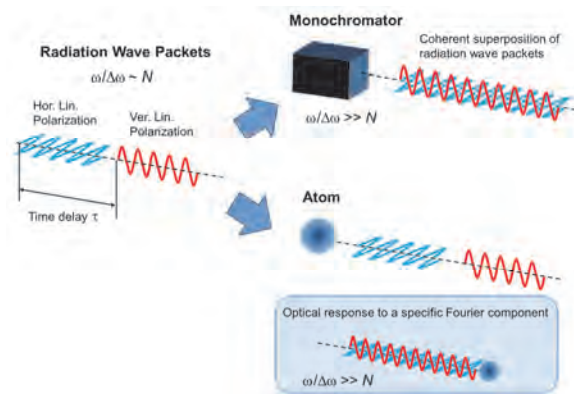

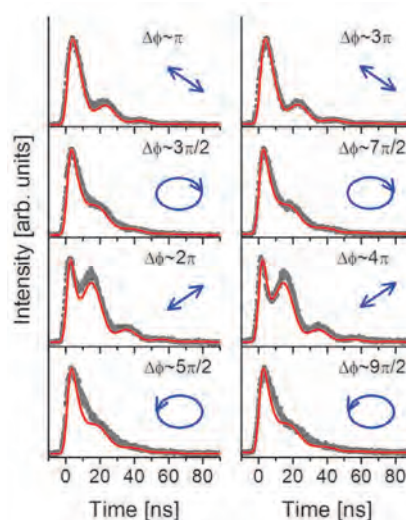Fig. 1. Polarization control in a crossed undulator.

Fig. 2. Zeeman quantum beat measured for fluorescence decay of 1s6p state. The gray circles and red curves represent measured and calculated results, respectively. The polarization ellipse and vectors assumed in the calculation are shown.

[1] T. Kaneyasu *et al.*, New J. Phys. **22** (2020) 083062.
[2] Y. Hikoska *et al.*, J. Synchrotron Radiat. **27** (2020) 675.

BL1U

Energy-Dependence of Photoelectron Circular Dichroism of Chiral Molecules

H. Kohguchi[1], Y. Hikosaka[2], T. Kaneyasu[3], S. Wada[1], M. Fujimoto[4], M. Katoh[4]
and Y-I. Suzuki[5]

[1]Graduate School of Advanced Science and Engineering, Hiroshima University, Higashi-Hiroshima 739-8526, Japan
[2]Institute of Liberal Arts and Sciences, University of Toyama, Toyama 930-0194, Japan
[3]SAGA Light Source, Tosu 841-0005, Japan
[4]UVSOR Synchrotron Facility, Institute for Molecular Science, Okazaki 444-8585, Japan
[5]School of Medical Technology, Health Sciences University of Hokkaido, Tobetsu 061-0293, Japan

Our group started a research project of photoelectron circular dichroism (PECD) of chiral molecules with BL1U beamline in 2020 February. Photoelectron scattering images exhibiting PECD, which appears as forward-backward asymmetry of the photoelectron angular distributions with respect to the propagation direction of circularly polarized light for ionization, have been measured for various typical chiral molecules. Methyl oxirane is one of the typical PECD molecules, by which we confirmed feasibility of our experimental setup to measure PECD [1]. In this research project, we have searched novel chiral species showing PECD.

We conducted theoretical calculations based on multiple scattering theory to predict the energy-dependence of PECD of polyaromatic molecules. The theoretical results of some chiral systems yielded a certain amount of PECD parameters (β_1) that are measurable with our experimental setup consisted of a velocity-mapping imaging (VMI) apparatus with the undulator light source at BL1U. Availability of samples is practically important for PECD study since each enantiomer is required for measurement. Most of promising candidates found in terms of theoretical β_1 values and availability were solid compounds at room temperature. We used a gas inlet nozzle with a heater to introduce isolated chiral molecules into the vacuum chamber. An example of the result (dimethyl binaphthyl) is shown in Fig. 1; mass signals of the higher mass > 60 amu with elevated nozzle temperature served as a good monitor for gas-phase samples in the detection zone. The photoelectron signal with irradiation of the VUV light increased as the growth of the high-mass peaks, indicating photoionization of the chiral molecules. We obtained the photoelectron images with a characteristic ring-like structure in the outer region (Fig. 2). The multiple rings, which could correspond to the band structure of the photoelectron spectrum, disappeared at the higher photon energy. The present experimental condition with linearly polarized light is applicable to the circularly polarization measurement. Additional calculation for the excited and ionized electronic states will provide an solid assignment of the photoelectron spectrum, which is a fundamental spectroscopic data for PECD measurements.
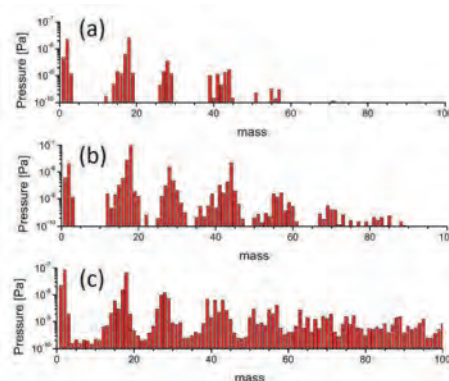

Fig. 1. Mass spectra of vaporized dimethyl binaphthyl at several nozzle temperatures with a heat nozzle. (a) room temperature, (b) nominal nozzle temperature of 50 °C, (c) 80 °C.
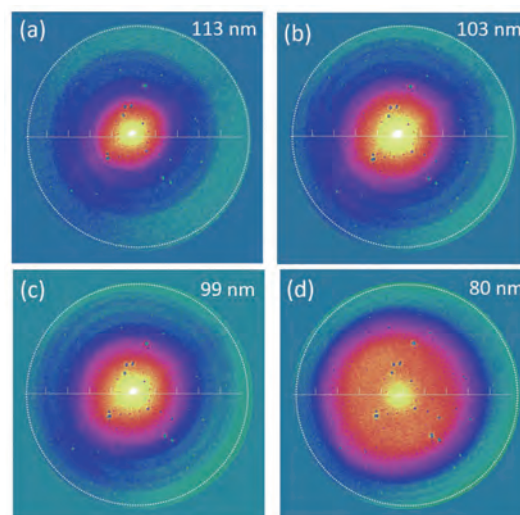

Fig. 2. Photoelectron images of dimethyl binaphthyl at several ionization wavelengths: (a) hν = 11.0 eV, (b) hν = 12.3 eV, (c) hν = 12.5 eV, (d) hν = 15.5 eV (expanded). White dotted circles define the detector edge.

[1] H. Kohguchi, Y. Hikosaka, T. Kaneyasu, S. Wada and Y-I. Suzuki, UVSOR Activity Report 2019 **47** (2020) 107.

BL1B, BL6B

Low-Frequency and THz Region Spectroscopy on Various Organic Molecules to Elucidate Microwave-Enhanced Organic Reactions

H. Takaya[1], K. Tanaka[2], F. Teshima[2], T. Yamada[3], M. Nishioka[4] and K. Kashimura[4]

[1]International Research Center for Elements Science, Institute for Chemical Research, Kyoto University, Uji 611-0011, Japan
[2]UVSOR Synchrotron Facility, Institute for Molecular Science, Okazaki 444-8585, Japan
[3]Faculty of Science and Engineering, Keio University, Yokohama 223-8522, Japan
[4]Faculty of Engineering, Chubu University, Kasugai 487-0025, Japan

THz and Low-frequency region spectroscopic analysis was performed on various organic compounds to investigate the dynamic behavior of organic molecules under microwave (MW) irradiation.

MW-enhanced chemical process has been recently focused intensely because the high-speed and high-selective molecular conversion provide a highly efficient chemical processes which never accessible by using the conventional heating techniques such as oil bath and electric heater. In this research, we conducted development of a BL1B/BL6B-based terahertz spectroscopic system which can be used under microwave irradiation to detect the molecular dynamics under oscillating electromagnetic field.

Our research group found that various organic and inorganic reactions can be drastically accelerated under microwave irradiation with high selectivity and low energy consumption. For direct observation of the MW-induced molecular dynamics in these reactions by THz spectroscopy at BL1B/BL6B, we designed a in situ THz measurement system as shown in Fig 1 (left),

where a newly developed small size MW resonant cavity is inserted into the optical path of sample chamber of 1B. As shown in the picture of Fig 1 (right), the setting of MW resonant cavity having a pair of light path port was succeeded to detect reference THz light under MW irradiation condition. We also designed PEEK-made sample holder where a low-dielectric loss factor material of PEEK is almost transparent toward MW with negligible absorbance at 2.45 GHz frequency of MW.

In the 2021 research project, we planed to perform in situ THz spectroscopic experiments using this system to investigate the effects of microwaves on 1) the racemization reaction of biaryl compounds where the racemization proceeds intramolecularly through the rotation around the biaryl axial linkage and 2) microwave-specific selective heating of nitrobenzenes in toluene solution. First of all detection of characteristic absorption bands (peaks) induced by MW irradiation will be the main goals of this project.
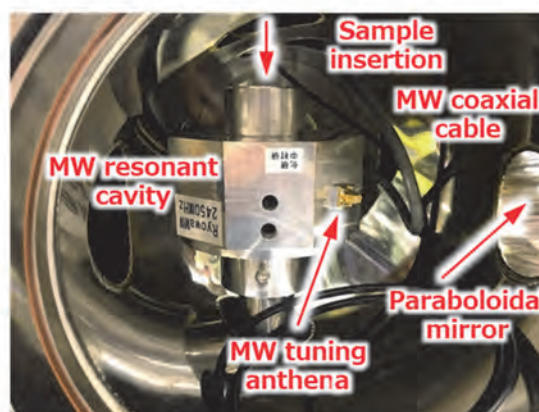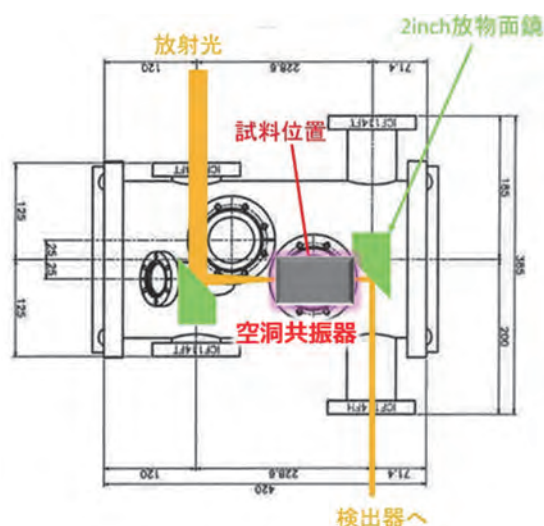

Fig. 1. The layout of microwave reaction system in the measurement chamber of BL1B THz optic system (left) and a picture of MW resonant cavity with the related electrical system inserted in the chamber of BL1B (right).

BL3U

XAS Measurements for Sugar Molecules in Aqueous Solutions

T. Sasaki and D. Akazawa

Department of Complexity Science and Engineering, Graduate School of Frontier Sciences,
The University of Tokyo, Kashiwa 277-8561, Japan

In recent years, attention has been paid to biomass conversion using water or an ionic liquid as a solvent without using an organic solvent. There have been many studies on biomass-related compounds in solution, but there are few reports on their molecular theory. We have studied the conversion process by dehydration reaction of polyalcohol as models of sugar molecules and found that the solvation structure with water molecules and the interaction with protons are important for the reaction process [1,2].

The purpose of this study is to explore the solvation structure of sugar molecules in aqueous solution, which is important in the conversion process from cellobiose to glucose, that is typical of biomass conversion process using water or ionic liquids. Cellobiose, a disaccharide, is taken up as a model substance for cellulose, which is one of the starting materials in biomass conversion. Of these, cellobiose can be hydrolyzed by the ionic liquid 1-ethyl-3-methyl-imidazolium chloride (EmimCl) to produce glucose [3]. These are typical routes for obtaining useful compounds from cellulose. A typical biomass conversion and utilization of glucose can be facilitated by elucidating the solvation structures and conversion mechanisms for related compounds.

In aqueous solutions, the dependence of temperature, pressure, and acidity will be investigated to elucidate the roles of hydrogen bond networks and protons surrounding sugar alcohol molecules. For ionic liquid aqueous solutions, the effect of polarity and viscosity will be elucidated by investigating the ionic liquid carbon chain length dependence. In this way, the entire molecular mechanism of sugar alcohol conversion using aqueous solutions and ionic liquid solutions will be elucidated, and the possibility of a more efficient sugar alcohol conversion route will be explored.

XAS measurements for liquid samples were conducted at UVSOR BL3U using facilities developed by Nagasaka et al [4]. The liquid sample cell with Si_3N_4 membranes was adopted, where the thickness of the liquid layer was controlled by the He gas pressure around the cell. The photon energy was calibrated by using the C-K edge XAS spectrum of the proline thin layer.

Figure 1 shows C-K edge XAS spectra for glucose and cellobiose aqueous solutions with concentrations specified in the figure. Molecular dynamics calculations for the solutions and the XAS simulations are under way to interpret the XAS spectra to explore the solvation structures of sugar molecules.
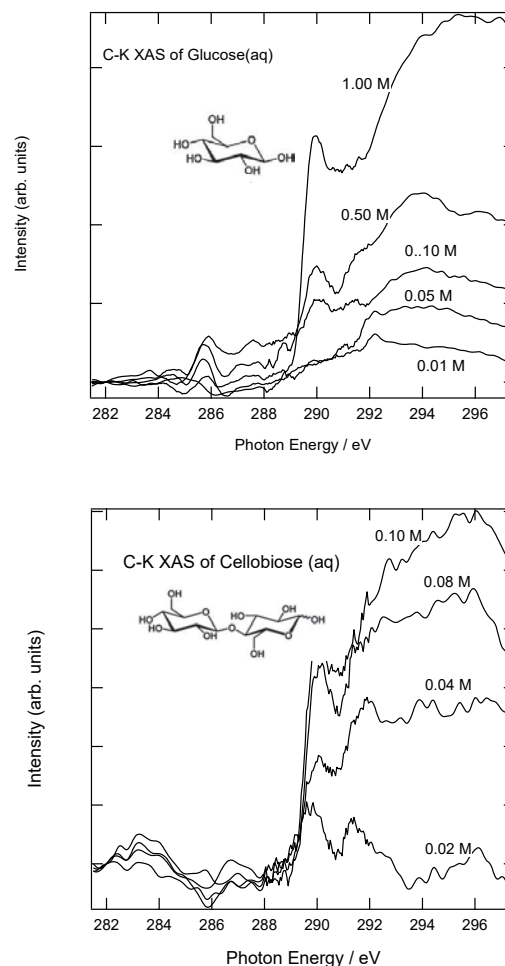

Fig. 1. C-K XAS spectra for glucose (upper panel) and cellobiose (lower panel) aqueous solutions.

[1] Y. L. Chang *et al*., J. Phys. Chem. B. **123** (2019) 1662.
[2] T. Kondo *et al*., J. Compuational Chem. **42** (2021) 156.
[3] Vanoyle *et al*., Green Chem. **11** (2009) 390.
[4] M. Nagasaka *et al*., J. Electrosc. Relat. Phenom. **200** (2015) 293.

BL3U

Nitrogen K-edge X-ray Absorption Spectroscopy of Metal Protoporphyrin IX Complexes in Aqueous Solutions

M. Nagasaka[1,2]

[1]Institute for Molecular Science, Okazaki 444-8585, Japan
[2]The Graduate University for Advanced Studies, SOKENDAI, Okazaki 444-8585, Japan

Iron porphyrin complex is a model of Cytochrome P450 that is important for enzyme reaction such as secondary metabolism. Chlorophyll *a* complex is used as a light-harvesting antenna for photosynthetic reaction. Thus, the electronic structural analysis of a metal complex is important for chemistry and biology. X-ray absorption spectroscopy (XAS) in the hard X-ray region extensively studied the electronic structures of central metals in metal complexes during a metal to ligand charge transfer process with photoirradiation [1]. The electronic structure of the central metal is also investigated by Fe L-edge XAS (700 eV) in the soft X-ray region [2]. Fe L-edge XAS is effective for the observation of the interactions between central metals and ligands since Fe L-edge is more sensitive for the measurements of valence and spin states than Fe K-edge in the hard X-ray region [3]. On the other hand, C and N K-edge XAS is necessary for investigating the electronic structures of ligands in metal complexes. Recently, Golnak et al. discuss the difference between liquid and solid states of hemin, which is also known as iron Protoporphyrin IX (FePPIX) complex, by using N K-edge XAS in fluorescence yield [4]. In this study, we have investigated interaction between metal and PPIX ligand from N K-edge XAS spectra of FePPIX, CoPPIX, and PPIX complexes in aqueous solution in transmission mode.

The experiments were performed by using a transmission-type liquid cell settled at BL3U [5]. The liquid layer is sandwiched between two SiC membranes and the liquid thickness is optimized to obtain appropriate absorbance of metal PPIX peaks. 50 mM FePPIX, CoPPIX, and PPIX in 0.5 M NaOH solutions were prepared. Although these complexes show dimer structure in aqueous NaOH solution, the interaction between metal and ligand would not be influenced in the dimer structures.

Figure 1 shows N K-edge XAS spectra of FePPIX, CoPPIX, and PPIX complexes in aqueous solutions. Sharp peaks around 398 eV and 400 eV are observed in the spectra of PPIX complex. In CoPPIX complex, the first peak shows a higher energy shift, and the second peak shows a lower energy shift compared to those in PPIX complex. These peaks are overlapped in the XAS spectrum. The XAS spectrum of FePPIX also shows same spectral features although the shoulder at the high energy side is smaller than that of CoPPIX. The peak around 403 eV in PPIX complex is also observed in CoPPIX complex, but it is not observed in FePPIX complex. In the future, we will discuss the

metal-ligand delocalization in metal PPIX complex more precisely with the help of quantum chemical inner-shell calculations.
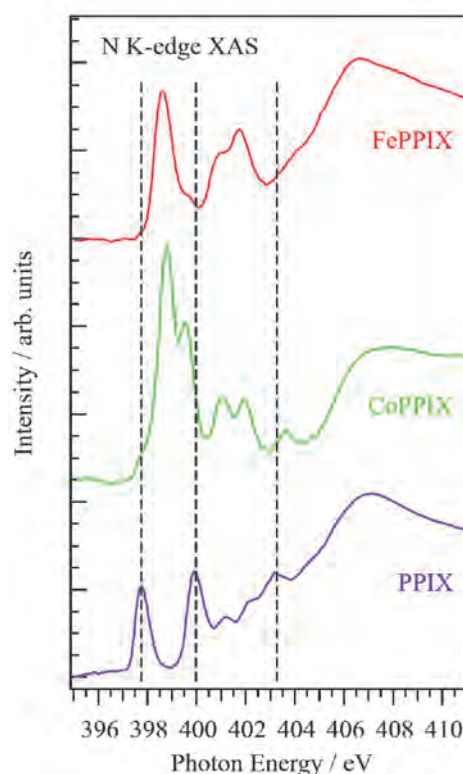

Fig. 1. N K-edge XAS spectra of FePPIX, CoPPIX, and PPIX complexes with the molar concentration of 50 mM in 0.5 M aqueous NaOH solutions. The dashed lines indicate the peak positions of PPIX.

[1] C. J. Milne, T. J. Penfold, M. Chergui, Coord. Chem. Rev. **277** (2014) 44.
[2] N. Huse *et al*., J. Am. Chem. Soc. **132** (2010) 6809.
[3] S. A. Wilson *et al*., J. Am. Chem. Soc. **135** (2013) 1124.
[4] R. Golnak *et al*., Phys. Chem. Chem. Phys. **17** (2015) 29000.
[5] M. Nagasaka, H. Yuzawa and N. Kosugi, Anal. Sci. **36** (2020) 95.

BL3U

XAS Study of a High Valent Oxo Species of a μ-Nitrido-Bridged Iron Phthalocyanine Dimer Deposited on a Graphite Surface

Y. Yamada [1,2,3] and M. Nagasaka [4]

[1]Department of Chemistry, Graduate School of Science, Nagoya University, Nagoya 464-8602, Japan
[2]Research Center for Materials Science, Nagoya University, Nagoya 464-8602, Japan
[3]PRESTO/JST, Kawaguchi 332-0012, Japan
[4]Institute for Molecular Science, Okazaki 444-8585, Japan

Methane has long been expected as a next-generation carbon resource because it is abundant in nature as natural gas or methane hydrate. However, its high C-H bond dissociation energy prevent the development of the catalyst that can convert methane into more valuable raw chemicals under mild reaction conditions. μ-Nitrido-bridged iron phthalocyanine dimer **1** (Fig. 1) is one of a few molecular catalysts for direct C-H activation of methane.[1,2] It is reported that treatment of **1** with H_2O_2 in an acidic aqueous solution produce high valent iron-oxo species **1oxo** possessing a strong methane oxidation activity. However, the electronic structure of **1oxo** have never been investigated by XAS presumably because of its high reactivity. In this study, we attempted to observe **1oxo** directly by XAS by using a highly oriented pyrolytic graphite (HOPG) substrate on which **1** was deposited (**1**/HOPG in Fig. 2(a)). We assumed that **1oxo** generated on a HOPG substrate is stable enough for XAS measurement as long as any organic substrates do not coexist.

Beforehand of this study, we confirmed that **1** was adsorbed on a highly oriented pyrolytic graphite to prepare **1**/HOPG successfully by treatment of a HOPG with the $1e^-$-oxidized monocationic species of **1** (**1**$^+$) in an organic solvent. O K-edge and Fe L-edge XAS measurements were performed at the soft X-ray beamline BL3U of UVSOR.[3] For these measurements, **1**/HOPG was fixed with double-sided conductive carbon tape onto a stainless sample holder. In order to generate **1oxo** on HOPG substrate, **1**/HOPG was treated with 35% aqueous H_2O_2 just before measurement. The holder with a HOPG sample was fixed on a rotatable linear and installed into a vacuum chamber ($< 1 \times 10^{-5}$ Pa). The XAS spectra were obtained in total electron yields by measuring a sample drain current.

Figure 2b shows a comparison of the O K-edge XAS spectra obtained for **1**/HOPG and **1**/HOPG treated with H_2O_2. It was found that the peak at around 532 eV was significantly increased after treatment with H_2O_2. DFT calculation for **1oxo** adsorbed on a graphene suggested that the peak assignable to the excitation of $O1s - \pi^*$ of Fe=O for **1oxo** should appear at around 529 eV, whereas the peaks for **1** with a coordinating H_2O on a graphene were calculated to appear at higher than 534 eV as shown in Fig. 2(c). On the other hand, Fe L-edge XAS spectra of **1**/HOPG after H_2O_2 treatment

showed slight high energy shifts compared to that before treatment. Taking that **1oxo** was observed by MALDI-TOF MS by using **1**/HOPG treated with H_2O_2, it is considered that the spectra shown in Fig. 2 indicates that **1oxo** was actually observed by XAS.
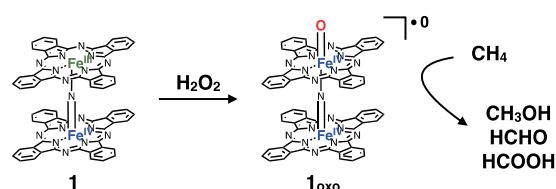

Fig. 1. Formation of a high valent iron-oxo species **1oxo** having methane oxidation activity.
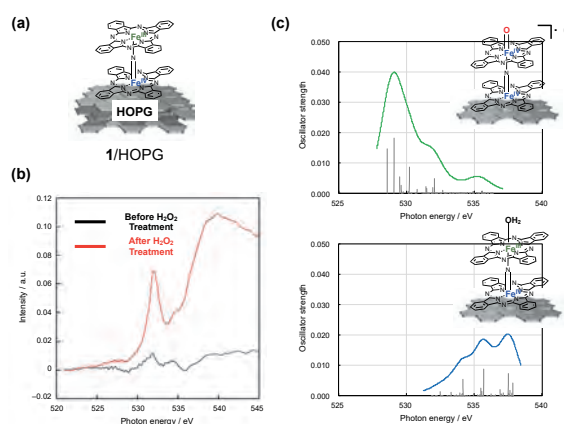

Fig. 2. (a) Structure of **1**/HOPG, (b) Comparison of O K-edge XAS spectra of **1**/HOPG before and after treatment with H_2O_2. (c) DFT-calculated O K-edge XAS spectra for **1oxo** on a graphene surface (upper) and **1**(OH_2) on a graphene surface (bottom).

[1] P. Afanasiev and A. B. Sorokin, Acc. Chem. Res. **49** (2016) 583.
[2] Y. Yamada, K. Morita, N. Mihara, K. Igawa, K. Tomooka and K. Tanaka, New J. Chem. **43** (2019) 11477.
[3] T. Hatsui, E. Shigemasa, N. Kosugi, AIP Conf. Proc. **705** (2004) 921.

BL3U

Mechanistic Investigation of Homogeneous Nickel-Catalyzed Organic Reactions Based on Solution-Phase L-edge XAS

H. Takaya[1,2], M. Nagasaka[2] and K. Kashimura[3]

[1]International Research Center for Elements Science, Institute for Chemical Research, Kyoto University, Uji 611-0011, Japan
[2]Institute for Molecular Science, Okazaki 444-8585, Japan
[3]Faculty of Engineering, Chubu University, Kasugai 487-8501, Japan

We have found that iron complexes of NiX_2 (phospine) (X =Cl or Br) bearing various phosphine ligands showed excellent catalytic activities toward the coupling of organometallic reagents of Mg, B, Al, and Zn with various aryl halides [1]. Such nickel-based catalysts for organic reactions alternative to the conventional precious metal catalysts has been intensively investigated for the development of future sustainable production of chemical compounds. Solution-phase XAS analysis is highly useful for the mechanistic study of iron-catalyzed organic reactions to identify the catalytically active organoiron species with their electronic and molecular structures, because the conventional solution-phase NMR analysis cannot be used due to the paramagnetic nature of organoiron species along with the large paramagnetic shift and peak broadening in NMR spectrum. L-edge XAS of transition-metal catalysts has been expected to be highly useful to investigate the electronic structure of 3d orbitals which provide essential information to elucidate how to work the catalyst. However, solution-phase L-edge XAS measurement is generally difficult because the measurement has to be performed under a vacuum condition where the solution sample is vaporized with vigorous boiling. In this project, we used the specially designed flow-cell for the solution-phase L-edge XAS measurement of homogeneous organic solution of nickel complex catalysts. In BL3U beamline, a stainless-steel flow cell has been used for various experiments, but we should carefully avoid contamination of iron species from the environment. For this reason Prof. Nagasaka newly designed and prepared PEEK-made flow cell bearing ultra-thin 100 nm Si_3N_4 membrane X-ray window (Fig. 1. left). The solvent-resistant PEEK made body worked well with an excellent chemical resistance toward the various organic solvents such as THF, CH_2Cl_2, toluene, and benzene, these often used in nickel-catalyzed coupling reactions. However, the static electrical charge generated by the frictional interactions between PEEK wall and organic solvents caused undesired baseline shifts in the NEXAFS spectrum. To solve this problem, a gold-made electrode was attached to the Si_3N_4 membrane with earth connection (Fig. 1. right). This flow cell was introduced into the He-filled chamber which inserted into the X-ray optics line, and connected to a syringe pump through a Teflon tube. The toluene solution samples of nickel phosphine

catalyst of $NiCl_2(PPh_3)_2$ **1** was prepared in an argon-filled glovebox, because the solution of iron complexes are quite sensitive to oxygen and water, and immediately react to give iron oxide and hydroxide. The XAS measurement was successfully carried out under a flow condition (flow rate: 50–200 μL/h) to give L-edge NEXAFS of **1** without the undesired baseline shift by the static electricity (Fig. 2.). However, the penetration of helium gas into the cell causing a bubbling noise could not be perfectly controlled. To solve this problem, Viton O-ring is changed to a fluorosilicone polymer with improving the flow line design and tube connection. This improved cell is testing in 2021 experiment.
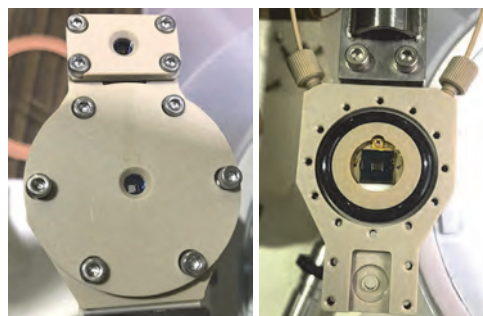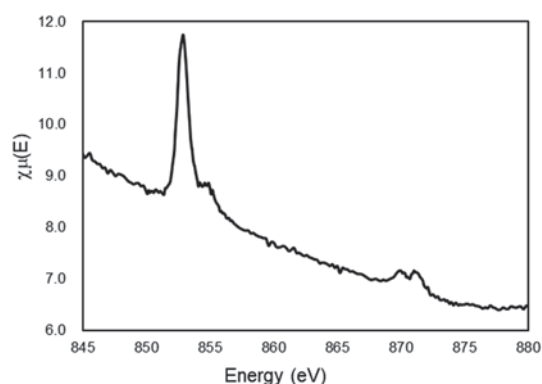

Fig. 1. Photos of the PEEK-made flow cell.

Fig. 2. Solution-phase L-edge XAFS spectrum of $NCl_2(PPh_3)_2$ in toluene.

[1] JP Patent 2020-016437 (Feb. 3, 2020).

BL3U

Complex Formation in Glycine Betaine Saline Solution Revealed by the Deconvolution of Its Soft X-Ray Absorption Band

S. Ohsawa[1], N. Fukuda[1], H. Iwayama[2,3], M. Nagasaka[2,3] and K. Okada[1,4]

[1]Graduate School of Science, Hiroshima University, Higashi-Hiroshima 739-8526, Japan
[2]Institute for Molecular Science, Okazaki 444-8585, Japan
[3]School of Physical Sciences, The Graduate University for Advanced Studies, SOKENDAI, Okazaki 444-8585, Japan
[4]Graduate School of Advanced Science and Engineering, Hiroshima University, Higashi-Hiroshima 739-8526, Japan

Living cells adapt to various environments, such as drought and high salinity, by regulating the concentration of solutes termed osmolytes [1], because an increase in extracellular salinity can cause water efflux and cell shrinkage. Among the most common organic osmolytes is glycine betaine. The amount of glycine betaine has been found to correlate with external salinity for several shoots of halophytes [2] and for halophilic eubacteria [3]. Altering the hydration structure of glycine betaine by salt addition presumably plays an important role in protecting the secondary structure of proteins, but the molecular level understanding of the hydration structure is not yet fully explored [4]. In this report O 1s absorption spectra were recorded for various concentrations of glycine betaine and sodium chloride, to extract the hydrated and bulk water components by a peak deconvolution technique.

Photoabsorption spectra of the solutions in the oxygen K-edge region were measured on the soft X-ray beamline, BL3U. A pair of windows made of thin silicon nitride membrane was used for the sample cell. The incident photon energy was calibrated to the peak at 530.88 eV of a polymer film [5]. Peak deconvolution was applied to the $4a_1$ resonance band of water into five components: one for the water hydrated to anions, three for the bulk water and one for the water hydrated to cations.

Figure 1 displays the peak area of the component for the water hydrated to cations versus the concentration of either glycine betaine or sodium chloride. The data for the betaine- and NaCl-only solutions align linearly, indicating the correctness of the present analysis. For mixed solutions of glycine betaine and sodium chloride, the data are plotted for the set of the varying NaCl concentration with the glycine betaine concentration constant (blue) and for the set of vice versa (green). The area for the former set decreases up to about 0.55 mol/dm³. The slope corresponds to the consumption of about 1.5 times the NaCl concentration. The decrease in area can be interpreted to be caused by the loss of water molecules hydrated to the solute due to the strong interaction between glycine betaine and sodium chloride. Above 0.55 mol/dm³ the area keeps nearly constant, which infers that different components of ion pairs exist in the solution. The data in green color behave similarly but have different slope. These results show that depending on the salt concentration the

betaine·Na⁺ complex with varying composition from 2:1 to 1:2 exists in glycine betaine saline solutions. We can therefore safely conclude that this provides the osmoregulation function in living cells against salinity.
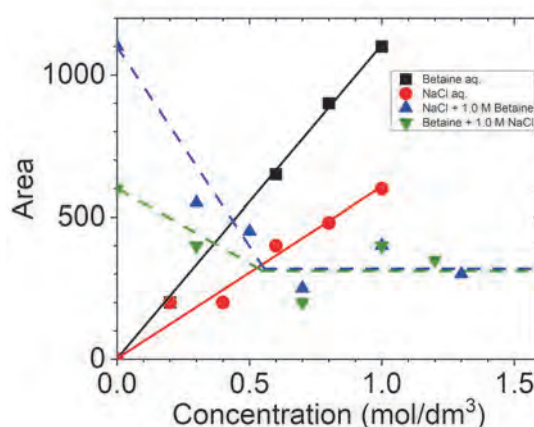

Fig. 1. Peak area of the water component hydrated to the sodium cation or cationic part of glycine betaine plotted against concentration.

[1] P. H. Yancey, M. E. Clark, S. C. Hand, R. D. Bowlus and G. N. Somero, Science **217** (1982) 1214.
[2] R. Storey and R. G. Wyn Jones, Plant Sci. Lett. **4** (1975) 161.
[3] J. F. Imhoff and F. Rodriguez-Valera, J. Bacteriol. **160** (1984) 478.
[4] S. Ohsawa, N. Fukuda, H. Iwayama, H. Yuzawa, M. Nagasaka and K. Okada, UVSOR Activity Report 2018 **46** (2019) 115.
[5] M. Nagasaka, H. Yuzawa, T. Horigome and N. Kosugi, J. Elec. Spectrosc. Relat. Phenom. **224** (2018) 93.

BL4U

Analysis of One-dimensional Single-crystalline Cathode Materials for Secondary Batteries by Scanning Transmission X-ray Microscopy

E. Hosono[1,2,3], W. X. Zhang[3,4], D. Asakura[1,2,3], Y. Harada[3,4], H. Yuzawa[5] and T. Ohigashi[5,6]

[1]*Global Zero Emission Research Center, National Institute of Advanced Industrial Science and Technology, Tsukuba 305-8568, Japan*
[2]*Research Institute for Energy Conservation, National Institute of Advanced Industrial Science and Technology, Tsukuba 305-8568, Japan*
[3]*AIST-UTokyo Advanced Operando-Measurement Technology Open Innovation Laboratory (OPERANDO-OIL), National Institute of Advanced Industrial Science and Technology (AIST), Kashiwa 277-8565, Japan.*
[4]*Institute for Solid State Physics, The University of Tokyo, Sayo 679-5148, Japan*
[5]*UVSOR Synchrotron Facility, Institute for Molecular Science, Okazaki 444-8585, Japan*
[6]*School of Physical Sciences, The Graduate University for Advanced Studies, SOKENDAI, Okazaki 444-8585, Japan*

Development of innovative technologies for clean energy devices is desired to realize sustainable society with preventing global warming, and development of high-performance secondary batteries for electric vehicle applications and grid introduction through large-scale power storage in renewable energy power plants is attracting much attention.

In secondary battery materials, when Li or Na ions diffuse into or out of the host crystal, the crystal axis along the diffusion path becomes clearer. However, the redox reaction is still unclear. The electronic-structure change in transition metals and oxygen of the host crystal due to the insertion or extraction of Li or Na in the single-crystal active material should be unveiled in detail. It is desirable to clarify the distribution of the electronic state using a position sensitive analysis with high spatial resolution. The knowledge of Li or Na diffusion with the electronic-structure change of the host structure is important for the understanding of cathode materials for secondary batteries from a viewpoint of basic science.

These discussions are directly related to the crystal structure change (volume change) and charge-discharge cycle characteristics related with fast ionic diffusion. If we clarify the battery characteristics from the electronic state, we can establish a strategy for innovative material design.

Here, we show a result of STXM for $LiMn_2O_4$ single-crystalline nanowire. Figure 1 shows the STXM image measured with an excitation energy of 525 eV. Nanowire image of $LiMn_2O_4$ was obtained by STXM. An O K-edge absorption spectrum of a selected region is shown in Fig. 2. The pre-edge region from 528 to 534 eV is attributed to the Mn 3d-O 2p hybridization.

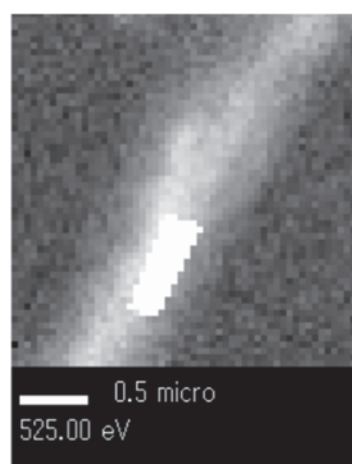In the near feature, we will establish *operando* STXM measurement system.

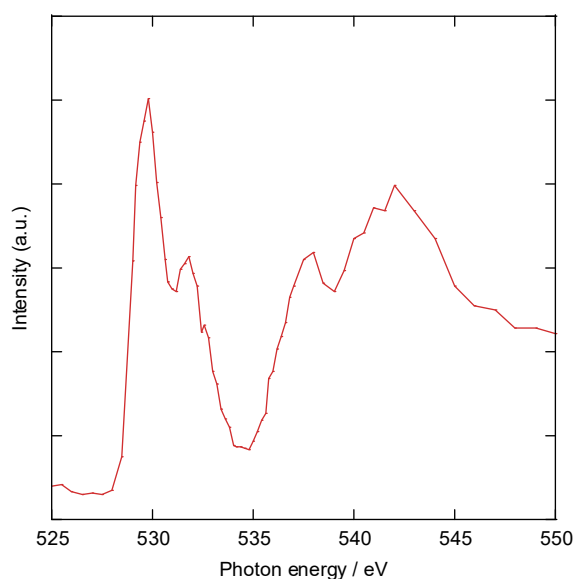Fig. 1. A STXM image of the $LiMn_2O_4$ single-crystalline nanowire.

Fig. 2. O K-edge absorption spectrum of a selected region.

BL4U

Analysis of High Active Photocatalytic Materials by Scanning Transmission X-ray Microscope

Y. Miseki [1,2], E. Hosono[1,3,4], D. Asakura[3,4], H. Yuzawa[5] and T. Ohigashi[5,6]

[1]Global Zero Emission Research Center, National Institute of Advanced Industrial Science and Technology, Tsukuba 305-8568, Japan
[2]Research Center for Photovoltaics, National Institute of Advanced Industrial Science and Technology, Tsukuba 305-8565, Japan
[3]Research Institute for Energy Conservation, National Institute of Advanced Industrial Science and Technology, Tsukuba 305-8568, Japan
[4]AIST-UTokyo Advanced Operando-Measurement Technology Open Innovation Laboratory (OPERANDO-OIL), National Institute of Advanced Industrial Science and Technology (AIST), Kashiwa 277-8565, Japan.
[5]UVSOR Synchrotron Facility, Institute for Molecular Science, Okazaki 444-8585, Japan
[6]School of Physical Sciences, The Graduate University for Advanced Studies, SOKENDAI, Okazaki 444-8585, Japan

The conversion of solar energy into chemical energy by artificial photosynthetic reactions is being studied as a candidate technology for realizing a sustainable low-carbon society. For the widespread use of this technology in society, it is important to establish design strategy for innovative photocatalytic materials that are significantly superior to the current performance. Since the photocatalytic reaction proceeds by redox reaction at the interface, it is necessary to establish appropriate design method for the reaction field, especially technology to control the crystallinity and crystal plane of the material.

However, since each catalytic material has a different active surface, it is important to confirm which surface is the active surface, as a preliminary step for precise control. Comparing the electronic states of the active surface with those of other surfaces and element-selectively/orbital-selectively understanding the mechanism of high activity is expected to lead to design strategy for the development of innovative materials.

To establish the high-level crystal growth techniques and morphology control methods, theoretical understanding from a viewpoint of electronic structure by using synchrotron radiation soft X-rays is necessary. Scanning Transmission X-ray Microscope (STXM) is most suitable to reveal the electronic structure information with spatial information (minimum spatial resolution is ca. 30 nm).

We have tried the preparation of *operando* measurement system for crystal growth in STXM. Figure 1 shows the optical microscope image of Mn^{2+} solution with agar gel sandwiched by Si chips with Si_3N_4 windows. One of the major features of STXM is that it is possible to obtain a spectrum of the solution by sandwiching it between the Si_3N_4 windows.

Figure 2 shows the spectrum of Mn. In the near feature, we will establish in-situ measurement system.
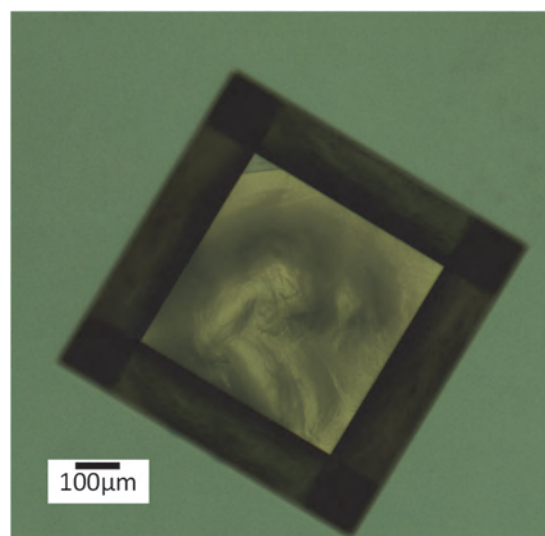

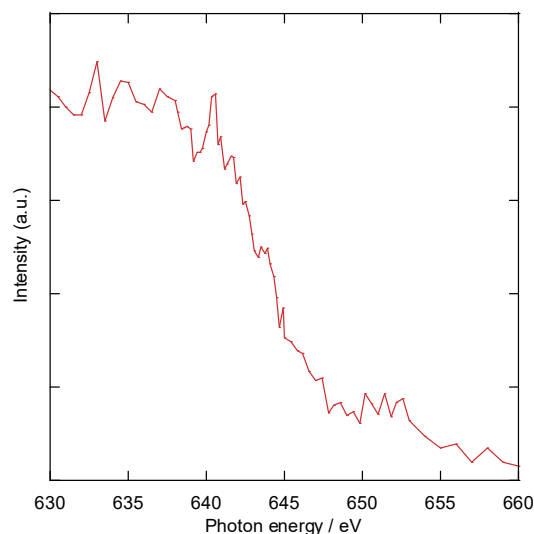Fig. 1. Optical microscope image of Mn solution with agar gel.

Fig. 2. Absorbance spectrum of Mn.

BL4U

Chemical State Mapping of a Heterostructured Oxygen Catalyst using STXM

J. Wang, J. Chung and J. Lim

Department of Chemistry, College of Science, Seoul National University, Seoul, 08826, Republic of Korea

Water electrolysis is regarded as one of the most promising methods for clean hydrogen production [1], where the sluggish kinetics of oxygen evolution reaction (OER) at the anode of a water electrolyzer compromised the energy efficiency [2]. For the purpose of boosting the OER rate, we proposed a new heterostructured OER catalyst by mating MoS_2 dichalcogenide with layered $LiCoO_2$ oxide. The as-prepared hybrid catalyst (MML) outperformed the commercial RuO_2 in catalyzing the OER and demonstrated remarkable stability. However, it is well known that both MoS_2 and $LiCoO_2$ are inert in OER activity. In order to look into the mechanism behind the synergistic performance enhancement, we applied scanning transmission X-ray microscopy (STXM) with several in-situ/ex-situ techniques to probe the dynamic structural change and to clarify the actual active species of the catalyst during the reaction.

The chemical state of MML sample before and after the OER was mapped around the Co L-edge and Mo M-edge at the BL4U beamline of the UVSOR. Hybridization with MoS_2 was found to lower the Co valence state of $LiCoO_2$, as clearly visualized from the mapping in Fig. 1 and supported by the representative line-cut spectra showing the negative shift of the Co L-edge spectrum of MML relative to that of pristine $LiCoO_2$. In addition, the homogenous distribution of Co valence states within the MML particle suggested the thorough mixing of the MoS_2 and $LiCoO_2$ components, which is expected to be beneficial to maximize the heterointerface density and tune the electronic structure. The maintenance of Mo in MML is confirmed by the Mo M-edge spectrum. However, it is challenging to judge the Mo valence state change from this soft XAS spectrum. To supplement this Mo data, XAFS around the K-edge was scanned, which demonstrated the reduced Mo in MML. From the oxygen K-edge spectrum, the hybridization of MoS_2 with $LiCoO_2$ led to the formation of oxidized oxygen moieties, which can be explained by the coordination of Co with S after the hybridization. Replacement of oxygen with less electronegative ligands (i.e., S) potentially activated the oxygen redox.

The MML sample after the catalysis was also investigated. From the valence state mapping, Co was oxidized during the OER, leading to a higher valence state. The oxidized Co in $LiCoO_2$ was accompanied by the leaching of Li, which process led to the structural reconstruction of $LiCoO_2$ forming the cobalt

oxyhydroxide. This deduction was also supported by various other techniques including in-situ XAFS, online ICP-MS, post-mortem TEM, etc. Without forming the heterointerface, the surface of pristine $LiCoO_2$ was transformed into spinel $LiCo_2O_4$, resulting in an inferior OER activity. This work highlighted the role of heterointerface in modulating the dynamic structural reconstruction of catalysts during water electrolysis. The corresponding manuscript is under draft now and will be submitted soon.
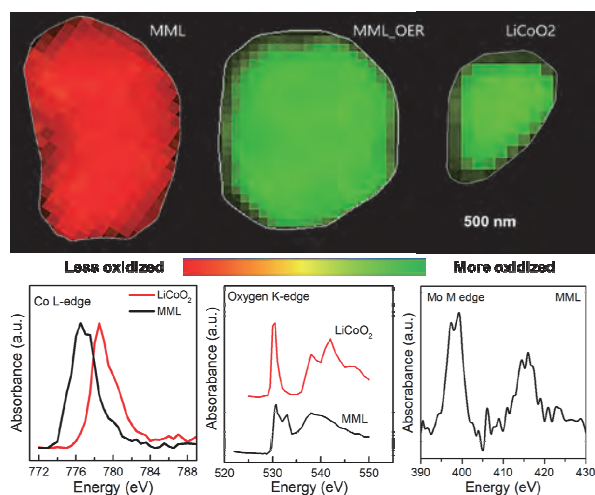

Fig. 1. Chemical state mapping around the Co L-edge of MML particle before and after the OER. A $LiCoO_2$ particle is also provided as a reference. The representative line-cut spectra of the MML sample around the Co L-edge, O K-edge, and Mo M-edge are shown below.

[1] Wang J, Gao Y, Kong H, Kim J, Choi S, Ciucci F, Hao Y, Yang S, Shao Z, Lim J. Chem. Soc. Rev. **49** (2020) 9154.
[2] Wang J, Kim SJ, Liu J, Gao Y, Choi S, Han J, Shin H, Jo S, Kim J, Ciucci F, Kim H, Li Q, Yang W, Long X, Yang S, Cho S, Chae K. H, Kim M. G, Kim H, Lim J. Nat. Catal. (2021) https://doi.org/10.1038/s41929-021-00578-1.

BL4B

Detection Efficiency of a Funnel MCP Estimated for Its Use in a Magnetic Bottle Electron Spectrometer

Y. Hikosaka

Institute of Liberal Arts and Sciences, University of Toyama, Toyama 930-0194, Japan

Magnetic bottle electron spectrometer, utilizing an inhomogeneous magnetic field to capture electrons formed by photoionization, is a very efficient electron spectroscopic tool and enabling one to perform multielectron coincidence spectroscopy very effectively. The electrons captured over 4π-steradian solid angle are guided to a detector (usually a microchannel plate (MCP) detector) ending a long flight path. Ions formed together with electrons can be detected with the same detector, by applying a pulsed electric field to the photoionization region [1-3]. The ion detection capability thus added to a magnetic bottle electron spectrometer leads to efficient coincidence measurements of multi-electrons and ions. The coincidence efficiency for the multiple particles is the product of the detection efficiencies for individual particles. Thus, gaining higher detection efficiency for each particle is crucial in achieving more effective coincidence measurements.

A standard MCP detector of 32-mm active diameter and 60% open area ratio had been employed in our previous multielectron-ion coincidence measurements [3]. For the electron detection, the coincidence efficiency limited by the detection efficiency of the MCP was practically observed [3,4]. In this work, we have newly introduced an MCP detector (40-mm active diameter) consisting of funnel micropores, instead of the previous one. The MCP has a large open area ratio (90%), and high detection efficiencies for electrons and ions are expected.

The detection efficiency of the funnel MCP for detections of electrons and ions was estimated on its use in the magnetic bottle electron spectrometer. A single mesh of 88% transmission was placed in front of the MCP, to avoid a leak of the electric potential of the MCP front. The electron detection efficiency, estimated from the number of Auger electrons from Ar 2p core-hole measured in coincidence with the relevant 2p photoelectron, is presented in Fig. 1 as a function of kinetic energy. The electron detection efficiency, observed to be constant around 0.7, is quite favorable, though it does not reach the open area ratio of the funnel MCP. The detection efficiency for ions, plotted in Fig. 2, was determined from the numbers of electrons ejected in known ionization paths in coincidence with the formed Xe ion. While the detection efficiency for the singly charged Xe ion is not very favorable on the present extraction pulse (2 kV height), those for highly-charged Xe ions are close to the value reflecting the open area ratio of the MCP. The present study proves that the use of the funnel

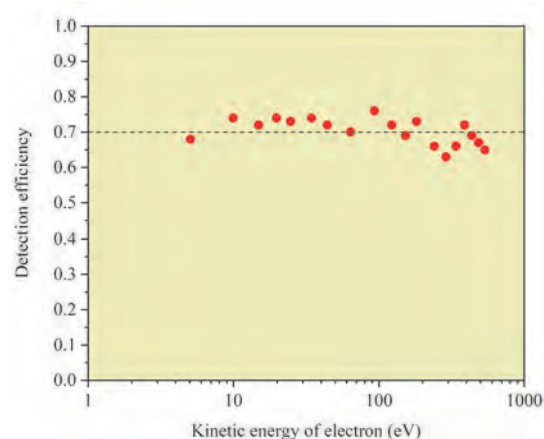MCP is promising in achieving more efficient multielectron-ion coincidence measurements.

Fig. 1. Electron detection efficiency of the funnel MCP estimated as a function of kinetic energy.
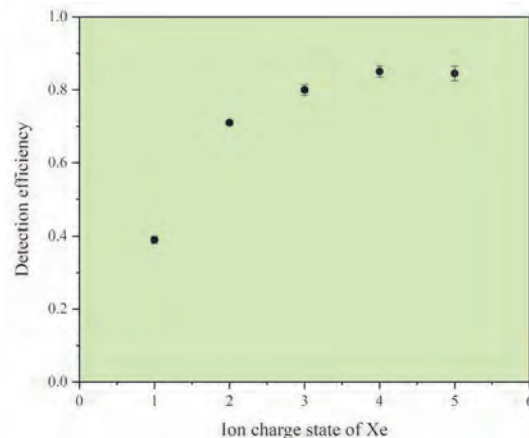

Fig. 2. Detection efficiency of the funnel MCP for Xe ions.

[1] A. Matsuda, M. Fushitani, C.-M. Tseng, Y. Hikosaka, J.H.D. Eland, and A.Hishikawa, Rev. Sci. Instrum. **82** (2011) 103105.
[2] J.H.D. Eland, P. Linusson, M. Mucke, and R. Feifel, Chem. Phys. Lett. **548** (2012) 90.
[3] Y. Hikosaka and E. Shigemasa, Int. J. Mass Spectrom. **439** (2019) 13.
[4] Y. Hikosaka, M. Sawa, K. Soejima, and E. Shigemasa, J. Electron Spectrosc. Relat. Phenom. **192** (2014) 69.